A Study of the $t\bar{t} + jets$ Background at LHC

Y.Q. Fang, B. Mellado, S. Paganis,
W. Quayle, Sau Lan Wu

Physics Department
University of Wisconsin - Madison
Madison, Wisconsin 53706, USA

Draft version3.0
30 March 2004

Abstract

A study of $t\bar{t}$ production at Next-to-Leading Order at $\sqrt{s} = 14$ TeV using the MC@NLO Monte-Carlo calculation is presented. A comparison between MC@NLO and standard Monte Carlo programs with Leading Order treatment of the hard process is performed. MC@NLO predicts a dramatic increase of the hard radiation/jets which are not part of the decay of the $t\bar{t}$ system, when compared to PYTHIA. MC@NLO also provides a reasonable description of the subleading radiation. As an application, the MC@NLO $t\bar{t}$ production prediction is used to provide a control background sample for the Vector Boson Fusion $H \to WW \to ll\nu\nu$ channel. The sample obtained can be tested against data in the early stages of ATLAS data taking.

1 Introduction

At LHC the Next-to-Leading Order (NLO) prediction for $t\bar{t}$ production is $\simeq$ 700 pb allowing to study the top quark with very high statistics. However the $pp \rightarrow t\bar{t}$ + jets process is also a major background for Higgs searches. This is illustrated in table 1, where a list of Standard Model (SM) Higgs and beyond the Standard Model (BSM) Higgs processes which have $t\bar{t}$ + jets as a significant background is given.

Table 1: *$t\bar{t}$ +jets background for Higgs searches at LHC*

Process (SM Higgs)	$t\bar{t}$ background contribution
$pp \rightarrow WH \rightarrow Wb\bar{b}$	$t\bar{t} \rightarrow WWb\bar{b}$ 2nd-most dominant
$t\bar{t}\ H \rightarrow t\bar{t}\ b\bar{b}$	$t\bar{t}$ jj dominant
$H \rightarrow ZZ^* \rightarrow 4l$	$t\bar{t} \rightarrow WbW\bar{b}$ dominant
$H- > WW^*$ (VBF)	$t\bar{t} \rightarrow WWb\bar{b} \rightarrow l\nu l\nu + X$ dominant
$WH \rightarrow WWW^* \rightarrow l\nu l\nu l\nu$	$t\bar{t}$ dominant
Heavy $H \rightarrow WW \rightarrow l\nu jj$ (VBF)	$t\bar{t} \rightarrow l\nu jjb\bar{b}$
Heavy $H \rightarrow ZZ \rightarrow lljj$ (VBF)	$t\bar{t} \rightarrow l\nu jjb\bar{b}$ 2nd-most dominant
Process (BSM)	
SUSY: $t\bar{t}\ + h \rightarrow t\bar{t}\ b\bar{b}$	$t\bar{t}$ +jets
SUSY: $H/A \rightarrow \tau\tau$	$t\bar{t}$ +jets
SUSY: $b\bar{b}\ H/A \rightarrow \tau\tau$ (large $tan\beta$)	$t\bar{t}$ +jets
SUSY: $H/A \rightarrow t\bar{t}$	$t\bar{t}$ +jets dominant
SUSY: $b\bar{b}\ H/A \rightarrow b\bar{b}\ b\bar{b}$	$t\bar{t}$ +jets (needs to be checked)
SUSY: $H \rightarrow hh \rightarrow b\bar{b}\ b\bar{b}$,$b\bar{b}\ \tau\tau$	$t\bar{t}$ dominant or 2nd dominant
SUSY: $A \rightarrow Zh \rightarrow llb\bar{b}$	$t\bar{t}$ dominant for parts of the phase space
SUSY: $H^{\pm} \rightarrow cs$	$t\bar{t}$ +jets dominant
SUSY: $bg \rightarrow H^{\pm}t \rightarrow tb\ t$	$t\bar{t}$ +jets dominant

The reconstruction of the various Higgs channels and the contribution of the $t\bar{t}$ background listed in table 1 was studied in detail in the ATLAS TDR [1]. In these studies the $t\bar{t}$ production was treated at Leading Order (LO) within the PYTHIA5.7 event generator [2]. A NLO description of the $t\bar{t}$ matrix element matched with parton shower is expected to improve the understanding of the $t\bar{t}$ + 1jet background at LHC, for jet $E_T > 30 - 50$ GeV. In this note a study of the $t\bar{t}$ + jets production at LHC is presented.

In section 2 the single available full Monte Carlo (MC) calculation that incorporates $t\bar{t}$ at NLO, MC@NLO is presented [3], and a comparison between MC@NLO and standard LO (at the Matrix Element) event generators PYTHIA6.2 [2] and HERWIG6.5 [4] is performed. In section 2 the MC@NLO description of the second jet from the $t\bar{t}$ + 2jets process is tested against a LO $t\bar{t}$ + 2jets Matrix Element calculation using Madgraph II [5]. In section 3 the MC@NLO $t\bar{t}$ production is used to define a $t\bar{t}$ + jets control sample for the specific Higgs production process $H \rightarrow WW \rightarrow ll\nu\nu$ via Vec-

tor Boson Fusion [6], [7]. This well defined control sample can be tested with data in the early stages of the ATLAS data taking at LHC. Such comparisons are expected to significantly reduce theoretical uncertainties in the background prediction for Higgs searches. In this analysis low luminosity LHC running was assumed ($10^{33} cm^{-2} s^{-1}$).

2 Monte Carlo Programs for $t\bar{t}$ + jets Production

The $pp \rightarrow t\bar{t}$ + jets production is currently calculated by the major MC programs PYTHIA6.2 [2] and HERWIG6.5 [4]. The problem with both of these MC event generators is that they use a Leading Order (LO) calculation of the $t\bar{t}$ production combined with a leading logarithmic (LL) treatment of higher orders as described by the Parton Shower (PS) approximation. The PS simulation provides a consistent treatment of the soft/collinear parton emissions but it provides a poor description of the hard emissions. This means that hard gluon radiation present at NLO could be missed and also that the $P_\perp$ distribution of the $t\bar{t}$ system could be completely wrong. In order to obtain a better treatment of the $t\bar{t}$ final state one would like to have an NLO treatment of the hard process matched to a parton shower prescription of the low $P_\perp$ region which is dominated by soft/collinear emissions. Such matching is non-trivial since parton showers include parts of the NLO corrections, which lead to the problem of double counting.

A recent attempt to combine NLO calculations and parton showers is the MC@NLO approach [3] which avoids double-counting and allows for a smooth matching between hard and soft/collinear emission regions. In MC@NLO hard emissions are treated as in NLO calculations while soft/collinear emissions are handled by the MC simulation (HERWIG 6.5 in this case) with the MC logarithmic accuracy: the $t\bar{t}$ + 1jet rates are known to NLO while the parton shower part preserves unitarity. In figure 1 sample graphs which are included in MC@NLO are presented. MC@NLO treats $t\bar{t}$ + 1jet at tree level, thus one loop graphs like the one shown in figure 2 are not included.

2.1 Comparison between MC@NLO, HERWIG and PYTHIA prediction of $t\bar{t}$ +1jet production

In this section a comparison of predictions between MC@NLO and the standard event generators HERWIG and PYTHIA is presented.

First we examine the $t\bar{t}$ system at the parton level. In fig. 3 we present the modulus of the vector sum of the transverse momenta of the t and $\bar{t}$ as predicted by PYTHIA, HERWIG and MC@NLO. While NLO calculations cannot predict the $P_\perp$ of the $t\bar{t}$ system at $P_\perp \simeq 0$ due to a logarithmic divergence, NLO is expected to give reliable predictions at high $P_\perp$. The parton shower approach as implemented in HERWIG and PYTHIA performs effective resummation at a transverse momenta of tens of GeV regulating

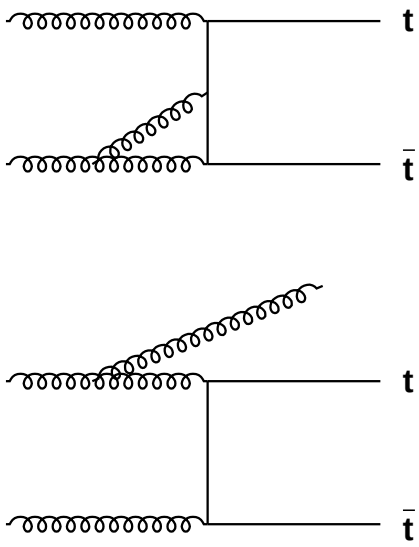

Figure 1: Example of graphs included in MC@NLO.

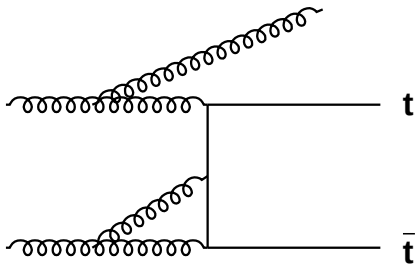

Figure 2: One loop $t\bar{t}$ + 1 jet graphs are not included in MC@NLO.

the infinity, however it is not expected to give reliable results in the high $P_\perp$ region. In fig. 3 one can see by comparing MC@NLO and HERWIG, a very good agreement

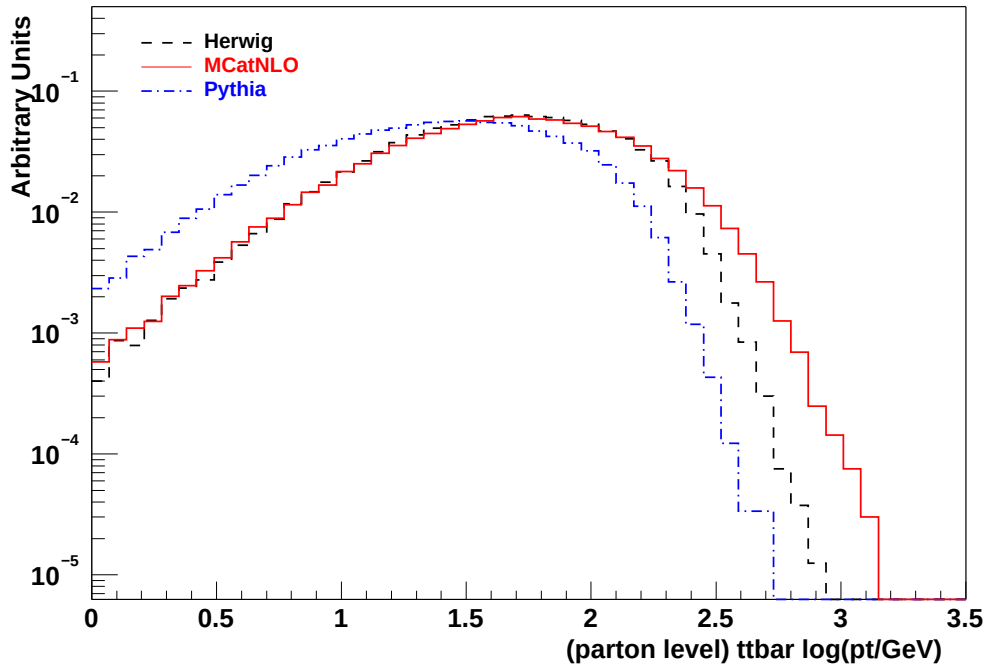

Figure 3: $P_\perp$ distibution of the $t\bar{t}$ system at the parton level as predicted by PYTHIA 6.2 (blue dotted-dashed line), HERWIG 6.5 (black dashed line) and MC@NLO (red solid line). All distributions are normalized to unity.

at low $P_\perp$ and a larger production of events with high $t\bar{t}$ $P_\perp$, for $P_\perp > 200$ GeV for MC@NLO. Within the MC@NLO approach the low $P_\perp$ region is dominated by the parton shower prescription while at higher $P_\perp$ the NLO calculation dominates predicting a significantly higher $P_\perp$ for the $t\bar{t}$ system. Surprisingly PYTHIA 6.2 largely disagrees with HERWIG predicting a much softer $P_\perp$ distribution. Final state radiation (from b-quark and light quarks) will not change the qualitative difference between HERWIG and PYTHIA.

In fig. 4 the distribution of the difference between the azimuthal angles of the t and $\bar{t}$, $\Delta\phi$, is presented. The small angle difference region $\Delta\phi \simeq 0$ is populated by configurations in which a hard jet recoils against the $t\bar{t}$ pair and by configurations in which t and $\bar{t}$ have small momenta. As shown in the figure, the MC@NLO predicts an increase of the small $\Delta\phi$ $t\bar{t}$ configurations due to the increase of high $P_\perp$ jets. The small t and $\bar{t}$ momenta configurations cannot be reliably described by an NLO calculation but in the case of MC@NLO the calculation is handled by the MC part (HERWIG).

Again PYTHIA disagrees with both HERWIG and MC@NLO predicting an almost back-to-back $t\bar{t}$ pair.

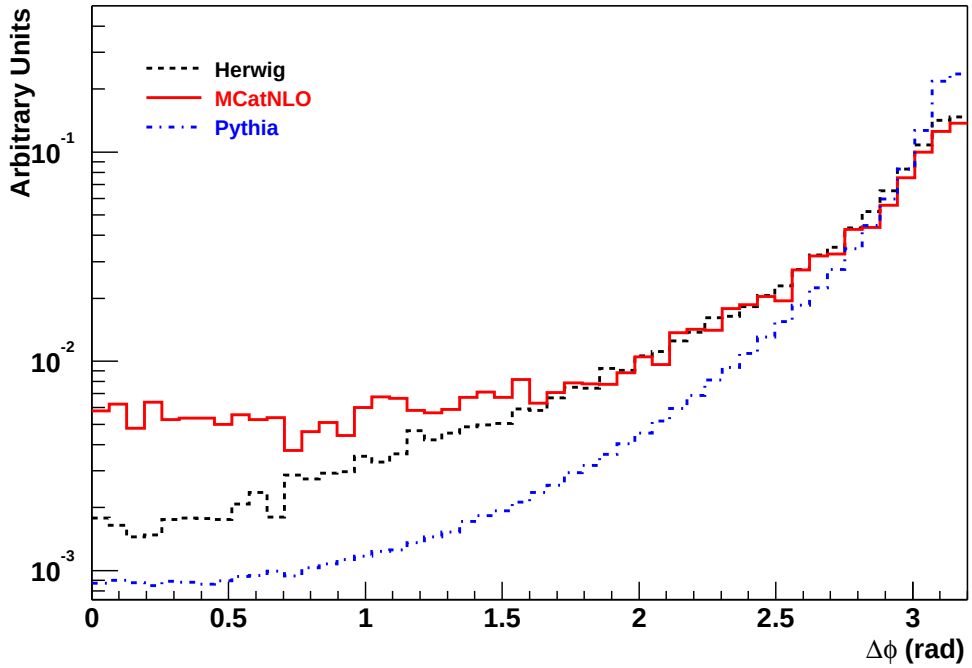

Figure 4: $\Delta\phi$ distibution of the $t\bar{t}$ system at the parton level as predicted by PYTHIA 6.2 (blue dotted-dashed line), HERWIG 6.5 (black dashed line) and MC@NLO (red solid line). All distributions are normalized to unity.

The output of the three event generators can be processed through the fast ATLAS reconstruction software ATLFAST [8]. The reconstructed leading jet $P_\perp$ is presented in fig. 5 for the three MC's. It is clear that the MC@NLO which is expected to provide a good description of the high $P_\perp$ region dominates for $P_\perp > 200$ GeV, while the MC part through the parton shower approach handles the low $P_\perp$ region. PYTHIA predicts a softer $P_\perp$ distribution with a difference of several orders of magnitude in the high $P_\perp$ region as compared to the NLO prediction. The $P_\perp$ distribution for the subleading jet is shown in fig. 6. As expected the distributions are softer but the same features as for the leading jet are observed.

One question that arises from the results presented above is on the origin of the hard jets predicted by the NLO. To find out if these hard jets originate from radiation from the hard process, one would like to study the b-jet $P_\perp$ distribution. If the extra hard jets originate from radiation then the NLO prediction for the b-jets (which originate from the $t\bar{t}$ pair) should not be significantly different from the LO prediction (HERWIG and

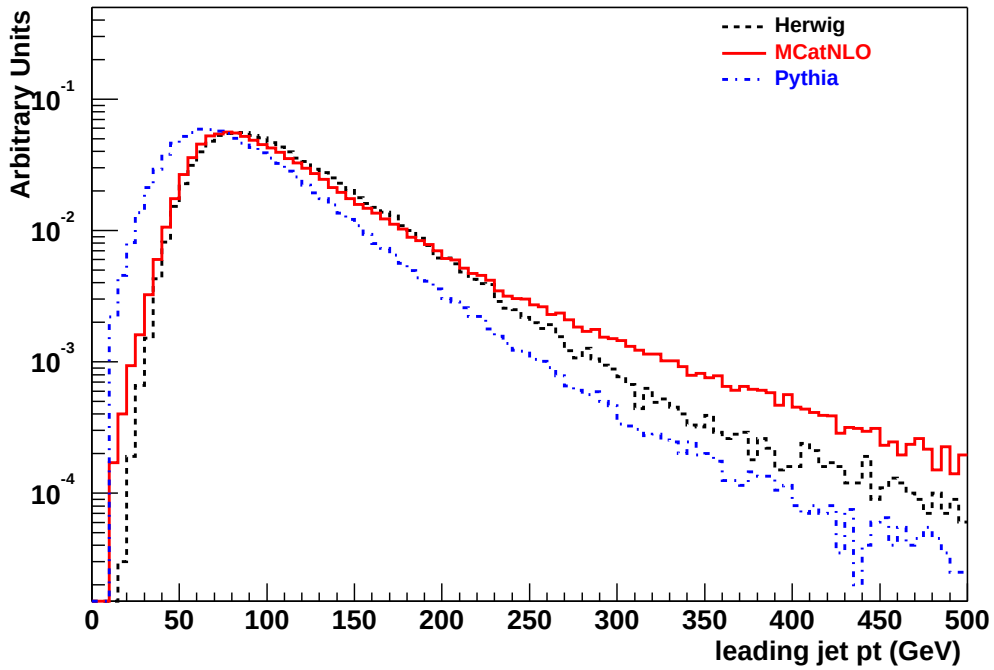

Figure 5: Leading Jet $P_\perp$ as reconstructed by ATLAS for three different MC's: PYTHIA 6.2 (blue dotted-dashed line), HERWIG 6.5 (black dashed line) and MC@NLO (red solid line). All distributions are normalized to unity.

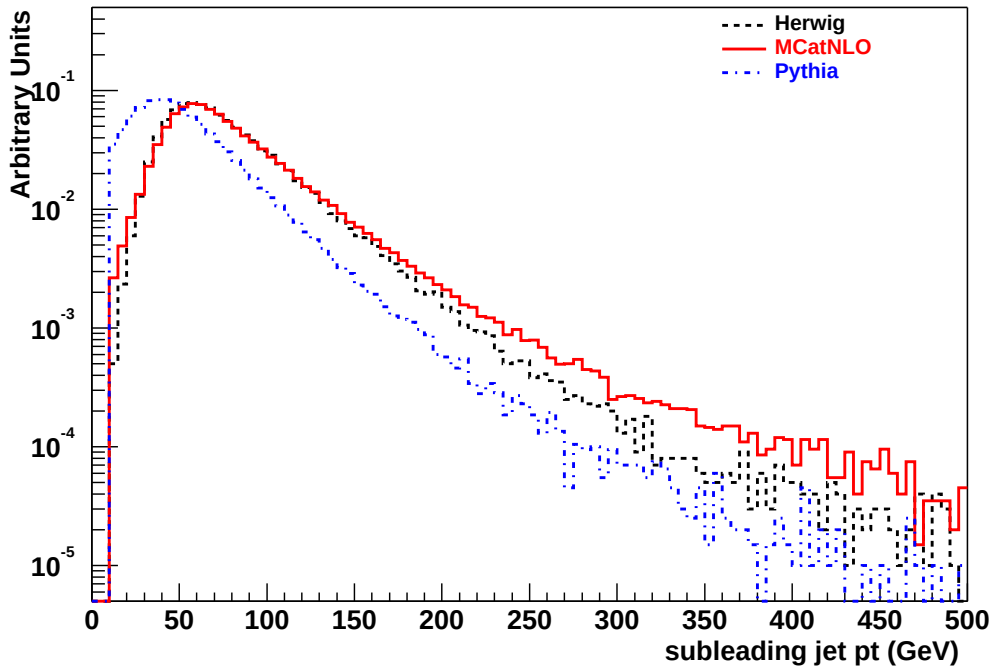

Figure 6: Subleading Jet $P_\perp$ as reconstructed by ATLAS for three different MC's: PYTHIA 6.2 (blue dotted-dashed line), HERWIG 6.5 (black dashed line) and MC@NLO (red solid line). All distributions are normalized to unity.

PYTHIA). This is shown in fig. 7 where the leading b-jet $P_\perp$ distribution is plotted. Not surprisingly one can see that all three MC's agree. This result shows that the origin of the extra hard jets predicted by the NLO is through radiation from the hard scattering parton lines (mainly gluons). This extra hard radiation is missed by the

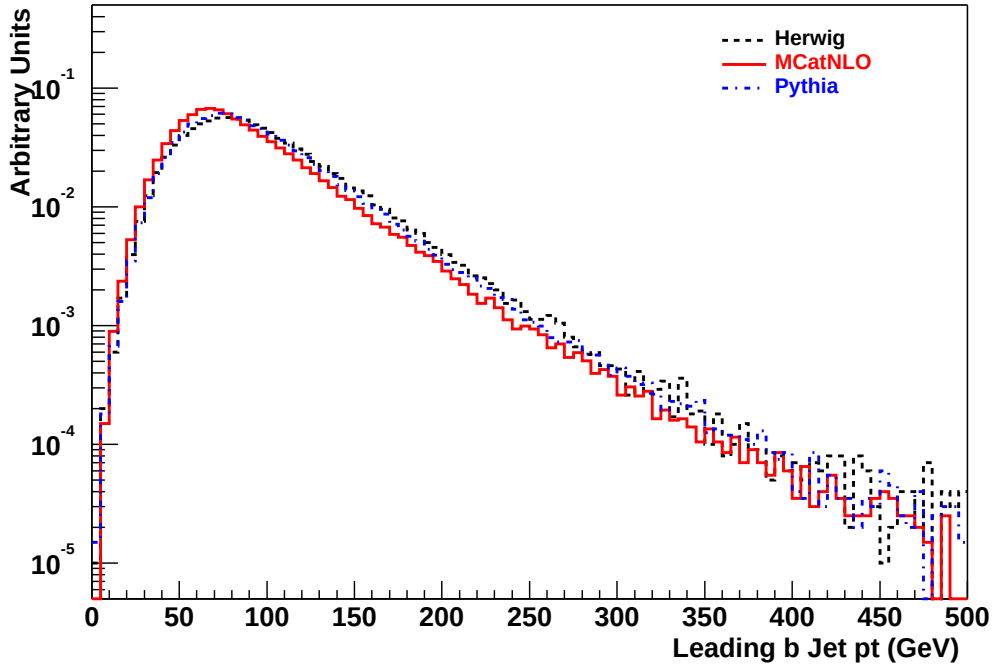

Figure 7: Leading b-Jet $P_\perp$ as reconstructed by ATLAS for three different MC's: PYTHIA 6.2 (blue dotted-dashed line), HERWIG 6.5 (black dashed line) and MC@NLO (red solid line). All distributions are normalized to unity.

parton shower approach. As an example, in HERWIG where angular ordering is used to deal with color coherence, there are "dead zones" in which hard radiation from the parton lines is suppressed. Within MC@NLO these hard emissions are expected to be properly handled by the NLO part.

2.2 Comparison between MC@NLO and Madgraph prediction of $t\bar{t}$ +2jet production

In the previous section it was shown that MC@NLO produces a leading jet in the final state which is dominated from radiation from the hard process. The production of this jet is at tree level. In the final state there may be more jets which are handled by the parton shower description. In this section we study the production of this second

jet within the MC@NLO generator. The appropriate basis of comparison would be a $t\bar{t}$ + 2jet Matrix Element calculation interfaced with an event generator which takes care of hadronization and avoids the problem of double-counting. Such a MC does not in principle exists, however standard MC generators like HERWIG provide interfaces to ME calculations which can be used with the risk of double counting at the overlapping regions between ME and the parton shower. MADGRAPH computes ME up to $2 \to 6$ at tree level for SM couplings. In this section we use MADGRAPH LO $t\bar{t}$ + 2jet Matrix Element interfaced to HERWIG and we compare the second jet MADGRAPH prediction with that of MC@NLO.

The method we use to perform the comparison is described below:

- Madgraph is normalized to MC@NLO using the leading non-b jet $P_\perp$ distributions.
- After normalization on the leading jet $P_\perp$, the subleading non-b jet $P_\perp$ distributions are compared at relatively high $P_\perp$ to avoid the region where the matrix element description fails.

In fig. 8 upper left plot, the normalized non-b jet $P_\perp$ distributions for $P_\perp > 100$ GeV for MC@NLO and Madgraph are shown. As expected there is a good agreement in the shapes since this $P_\perp$ range is dominated by the ME calculation. The comparison of $P_\perp$ distributions of the subleading non-b jet is shown in fig. 8 upper right plot, after normalization on the leading non-b jet. Clearly the two distributions disagree in the intermediate $P_\perp$ range $50 < P_\perp < 170$ GeV. A more careful examination of the Madgraph distribution shows a sharp drop in the $\simeq 170$ GeV region, i.e. very close to the top quark mass. In HERWIG the top quark mass sets the scale above which parton shower radiation is cut off. Consequently the sharp drop at this cutoff scale indicates the presence of double counting between ME and parton shower in the Madgraph-HERWIG interface. The pseudorapidity distributions of the leading and subleading non-b jets are shown in the lower plots of fig. 8.

To reduce the double-counting effect, the parton shower cutoff in HERWIG is reduced to the $P_\perp$ of the lowest $P_\perp$ QCD parton in the ME calculation. The resulting $P_\perp$ distribution comparison is shown in the upper plots of fig. 9. In this case the high $P_\perp$ tail of the Madgraph prediction (upper right plot) is a result of the matrix element calculation and should provide a reasonable description of the subleading non-b jet $P_\perp$. The new comparison shows that MC@NLO predicts a subleading non-b jet which is in good agreement for $P_\perp > 50$ GeV with the Madgraph $t\bar{t}$ + 2jet ME calculation. The disagreement for $P_\perp < 50$ GeV may come from the combined effect of residual double counting and divergence of the perturbative series.

In conclusion MC@NLO being a better implementation of QCD provides a reliable description of the leading non-b jet radiated from the hard scattering process. MC@NLO also provides a reasonable description of the subleading radiation which is mostly handled by the parton shower approximation.

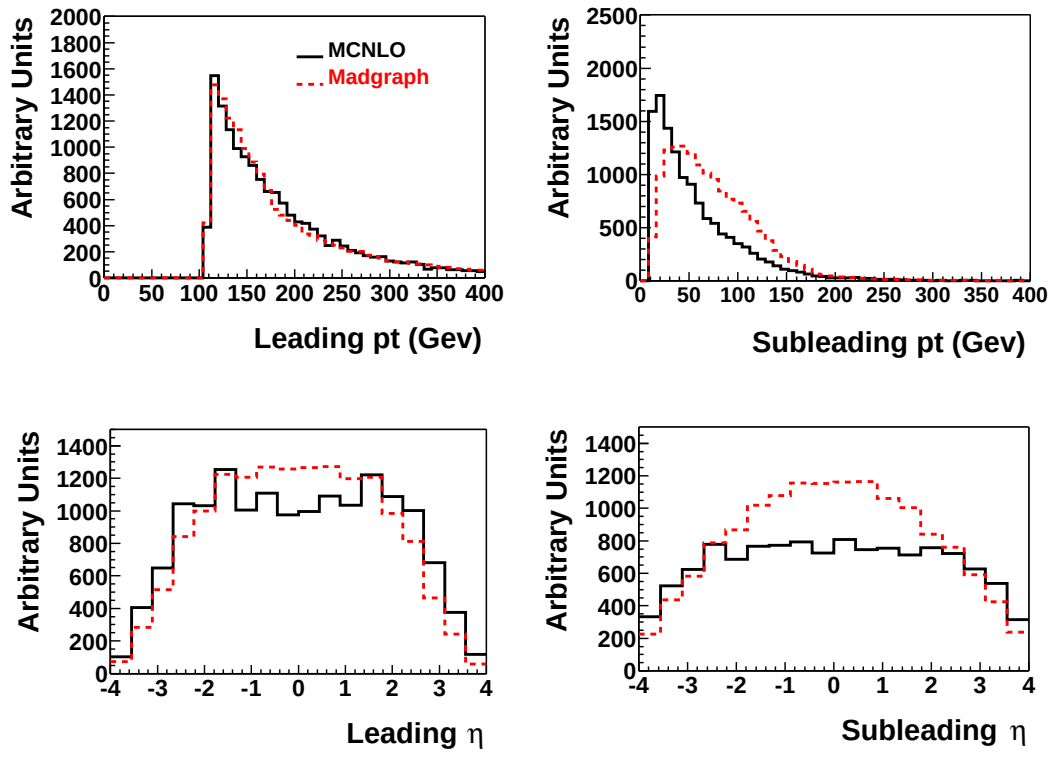

Figure 8: Normalized Madgraph and MC@NLO $P_\perp$ distributions of the leading non-b jet (upper left). Subleading non-b jet $P_\perp$ distributions after leading jet normalization (upper right). Pseudorapidity η distributions for leading (lower left) and subleading (lower right) non-b jet.

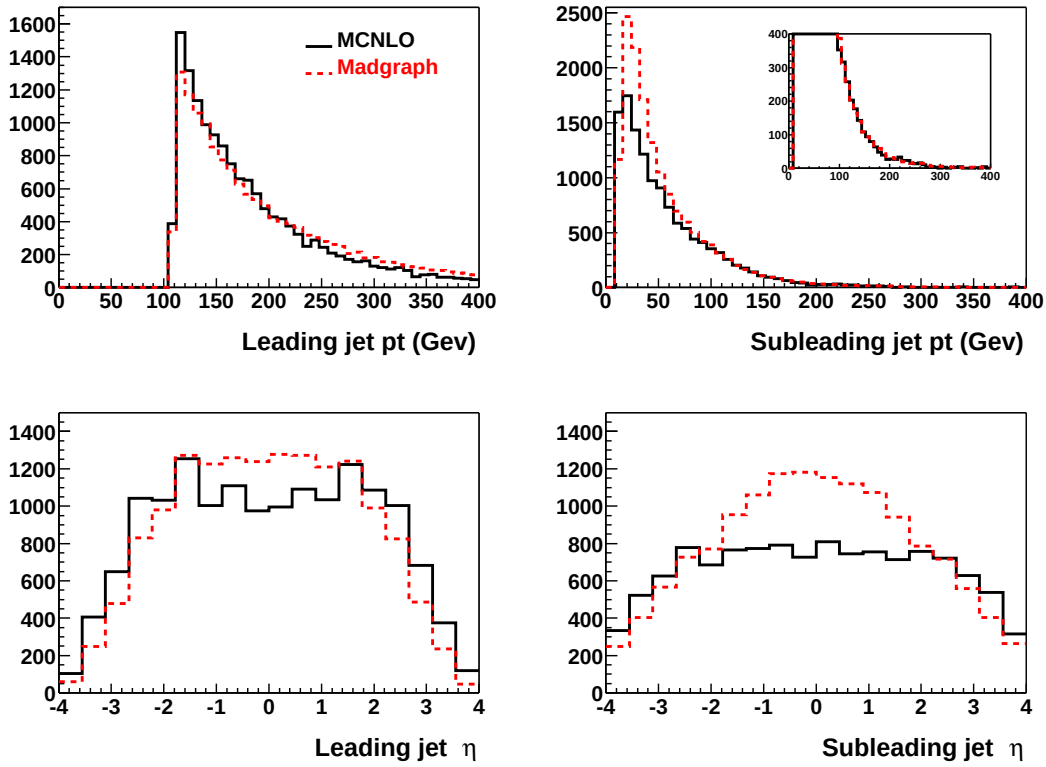

Figure 9: Normalized Madgraph and MC@NLO $P_\perp$ distributions of the leading non-b jet after lowering the parton shower cutoff scale for the Madgraph-HERWIG interface (upper left). Subleading non-b jet $P_\perp$ distributions after leading jet normalization (upper right). The level of agreement between the two MC's at high $P_\perp$ is shown in the inset. Pseudorapidity η distributions for leading (lower left) and subleading (lower right) non-b jet.

3 $t\bar{t}$ + jets Control Sample for the VBF $H \to WW^* \to ll\nu\nu$ channel

According to the results of the previous section MC@NLO provides a reliable description of the $t\bar{t}$ + 1jet and $t\bar{t}$ + 2jet production at LHC. A direct application of MC@NLO in the VBF $H \to WW \to l^+l^-\nu\nu$ channel at LHC is presented in this section. The reconstruction of this channel with ATLAS has been initially studied in [6] and more recently in [7]. The signature of the $H \to WW^* \to l^+l^-p_T^{MISS}$ VBF process, is two energetic forward jets (tagging jets), suppressed hadronic activitiy between the jets, large missing p_T and two oppositely charged leptons with large transverse momentum. The dominant background at LHC comes from the $t\bar{t}$ + jets production. In this process one may have the following background signatures:

1. $t\bar{t}$ + 0jets: the $t\bar{t}$ decays to a Wb pair and the W^+, W^- decay to two oppositely charged leptons. The $b\bar{b}$ produce a pair of b-jets which mimic the tagging jets from the Higgs decay.
2. $t\bar{t}$ + 1jet: in this case there are three jets in the final state, two of which mimic the tagging jets.
3. $t\bar{t}$ + 2jets: the two leading jets may mimic the tagging jets.

Parton level studies have shown that the $t\bar{t}$ + 1jet configuration comprises 80% of the total $t\bar{t}$ background contribution [9]. In this section MC@NLO is used in order to produce a $t\bar{t}$ + 1jet control sample for the VBF $H \to WW^* \to ll\nu\nu$ process. In this case the control sample is the $t\bar{t}$ + 1jet final state which most closely resembles the signal channel final state. Such a sample can be confronted with data in the early stages of ATLAS data taking and the results of the data versus MC comparison are expected to significantly reduce the uncertainties in the calculation of this dominant background. Before we present the generation of the control sample we briefly discuss the jet reconstruction method used.

3.1 Jet tagging and reconstruction

The $t\bar{t}$ final state was generated using MC@NLO. The ATLAS detector response was simulated by ATLFAST [8]. In this study it is essential to identify the true partonic origin of a reconstructed jet. In particular one would like to know if the jet is a b-jet, i.e. if the jet originates from the $t\bar{t}$ system. The method used to call a reconstructed jet a b-jet is to use a proximity radius $\Delta R = \sqrt{(\phi_{jet} - \phi_{b-quark})^2 + (\eta_{jet} - \eta_{b-quark})^2}$ in the pseudorapidity and azimuthal angle space. One has to be careful on the choice of ΔR: large ΔR decreases the purity of the b-jet sample by accepting non-b-jets; small ΔR reduces the efficiency in identifying b-jets. The optimum choice for ΔR was based on fig. 10. In this study a $\Delta R = 0.3$ cut is used.

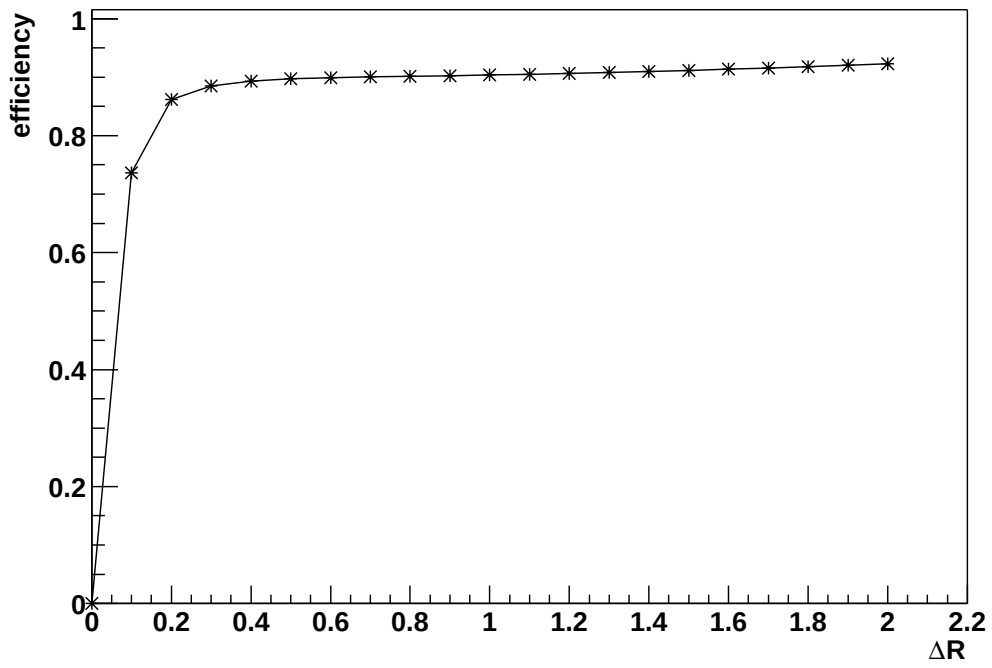

Figure 10: Fraction of b-jets identified using the true parton information through $\Delta R = \sqrt{(\phi_{jet} - \phi_{b-quark})^2 + (\eta_{jet} - \eta_{b-quark})^2}$ as a function of ΔR.

ATLFAST does not provide a realistic b-jet tagging efficiency. For this purpose the ATLFAST-B [8] package was used which provides an average $\simeq$ 60% b-jet tagging efficiency. The efficiencies for the three most energetic jets are shown in table 2.

Table 2: *Efficiencies of b-jet tagging of ATLFAST-B*

leading jet	subleading jet	third-leading jet
0.573237	0.612275	0.803418

Finally the jet energy as reconstructed from ATLFAST using HERWIG is underpredicted: reconstruction of the W mass through the $W \to jj$ channel is 11.9% lower than the true W mass. ATLFAST-B provides a correction which brings the W mass to 4.7% from its true value. A further correction which gives a smaller than 1% deviation from the W mass was applied by the authors for the purposes of this study.

3.2 The $t\bar{t}$ + jets Control Sample

For the definition of the $t\bar{t}$ + jets control sample a set of cuts similar to the ones used by Rainwater and Zeppenfeld [7] were examined:

- Two oppositely charged leptons with $P_\perp > 15$ Gev (10 Gev) for electrons (muons) and a two-lepton invariant mass $M_{ll} > 100$ GeV if both leptons are of the same flavor.
- Two tagging jets (most energetic jets) in opposite hemispheres with leading jet $P_\perp > 30$ GeV and subleading jet $P_\perp > 20$ GeV.
- Variable $|\Delta\eta|$ separation between the two tagging jets: $|\Delta\eta| > 2,\ 2.5,\ 3,\ 3.5,\ \ldots 6$ units of pseudorapidity.

The lepton invariant mass cut is used for Z background suppression. The separation in pseudorapidity between the tagging jets removes a large fraction of the $t\bar{t}$ background which tends to produce two leading jets with smaller separation than the signal. The efficiency of these cuts is presented in table 3. In [7] $|\Delta\eta| > 3.5$ was used as the optimum cut. From the results of table 3 we see that the general conclusions about the $t\bar{t}$ backround do not change and the same cut is still close to optimum.

The $t\bar{t}$ + jets background which survives the $|\Delta\eta| > 3.5$ cut, tends to produce a third jet between the two most energetic jets. A powerful cut which is expected to significantly reduce the $t\bar{t}$ + jets background is the central b-jet veto: events with a b-jet in the mid-rapidity region (for example $|\eta_{b-jet}| < 2.5$) are removed. In table 4 the efficiency of the standard cuts discussed above including a b-jet veto with $|\eta_{b-jet}| < 2.5$ as a function of $|\Delta\eta|$ between the tagging jets, is presented. The imprortant result here

Table 3: *Efficiency of $|\Delta\eta|$ cut and final cross section for different $|\Delta\eta|$* . The opposite electron cut efficiency is 0.327 and the tagging jets efficiency is 0.4317.

$\|\Delta\eta\|$	$\|\Delta\eta\|$ cut	final cross section (pb)
2	0.566516	3.52252
2.5	0.416945	2.59251
3	0.290863	1.80855
3.5	0.192996	1.20003
4	0.122365	0.760848
4.5	0.0726555	0.451763
5	0.040274	0.250419
5.5	0.0208328	0.129536
6	0.0102607	0.0638

Table 4: *Efficiencies of cuts including b-jet veto and final cross section with different $|\Delta\eta|$*

$\|\Delta\eta\|$	$\|\Delta\eta\|$ cut	final cross section (pb)
2	0.619827	0.88088
2.5	0.484112	0.692267
3	0.3571	0.512131
3.5	0.247651	0.354053
4	0.163622	0.233053
4.5	0.103851	0.148251
5	0.0606952	0.0871787
5.5	0.0339826	0.048312
6	0.0179858	0.0255493

is that the efficiency of the central b-jet veto cut is independent of $|\Delta\eta|$ and around 40%.

A summary of the results of tables 3 and 4 is presented in fig. 11.

It is crucial to understand if the central b-jet veto changes the topology of the $t\bar{t}$ + jets final state. This can be checked by examining the distribution of the fraction of events with the leading and/or subleading or third most energetic jet being a b-jet as a function of the tagging jet separation $|\Delta\eta|$. The fraction of events for which the leading jet is a b-jet before and after the application of the central jet veto is shown in fig. 12. The fraction of events for which the subleading jet is a b-jet before and after the application of the central jet veto is shown in fig. 13. The fraction of events for which the third most energetic jet is a b-jet before and after the application of the central jet veto is shown in fig. 14.

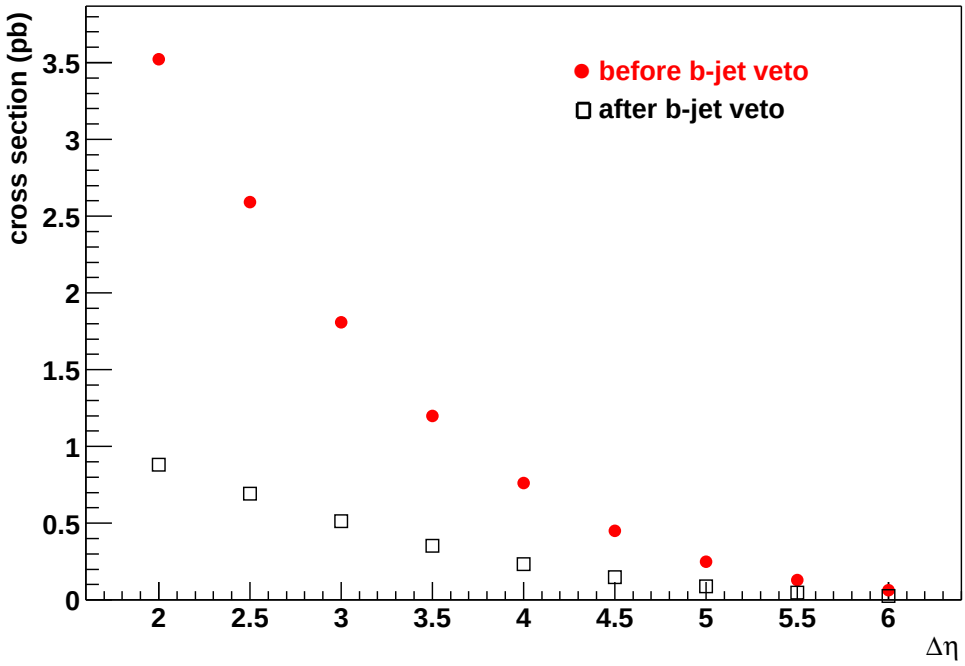

Figure 11: $t\bar{t}$ + jets cross section after selected cuts before (filled circles) and after (open circles) central b-jet veto as a function of the $|\Delta\eta|$ separation between the two tagging jets.

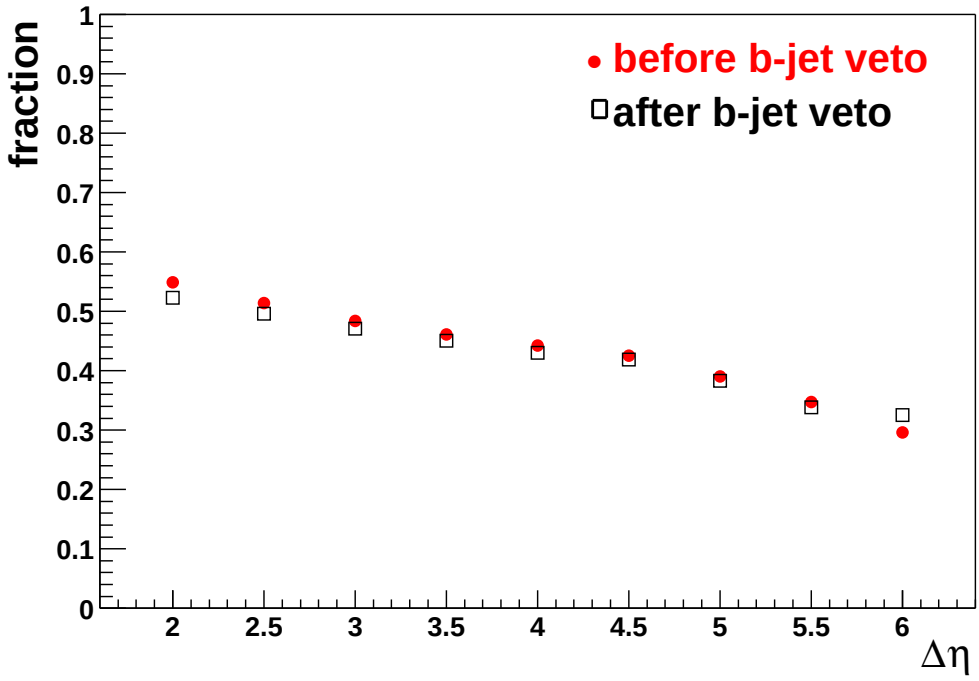

Figure 12: Fraction of events for which the leading jet is a b-jet before and after the application of the central jet veto as a function of $|\Delta\eta|$

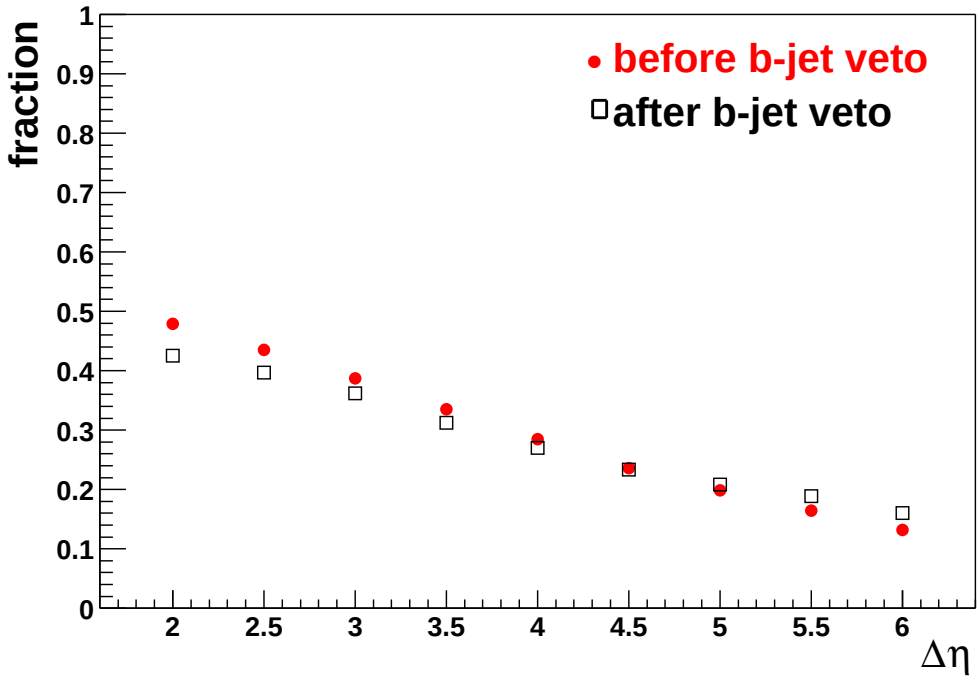

Figure 13: Fraction of events for which the subleading jet is a b-jet before and after the application of the central jet veto as a function of $|\Delta\eta|$

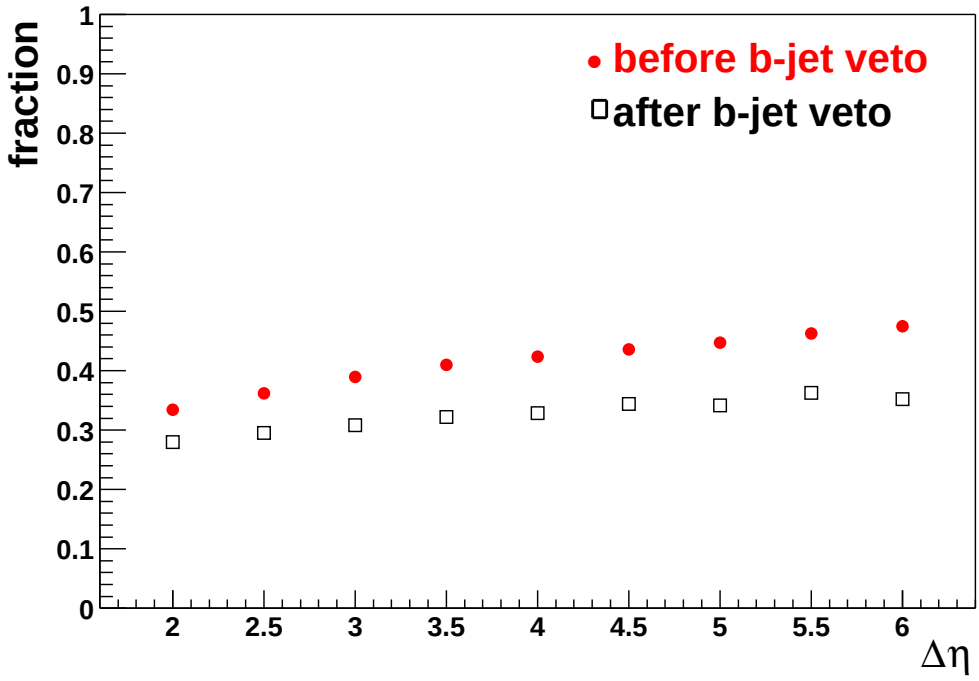

Figure 14: Fraction of events for which the third most energetic jet is a b-jet before and after the application of the central jet veto as a function of $|\Delta\eta|$

The fraction of events for which both leading and subleading jets are b-jets before and after the application of the central jet veto is shown in fig. 15. Clearly for small $|\Delta\eta|$ there is a large portion for which both leading jets are b-jets ($\simeq$ 20%). However, the dominant background for the VBF produced $H \to WW^* \to ll\nu\nu$ is $t\bar{t}$ + 1jet with one of the two leading jets being the extra (non-b) jet, and the third jet being a central b-jet. Thus a $|\Delta\eta|$ at least greater than 3 units is needed to select the background which most closely resembles the signal.

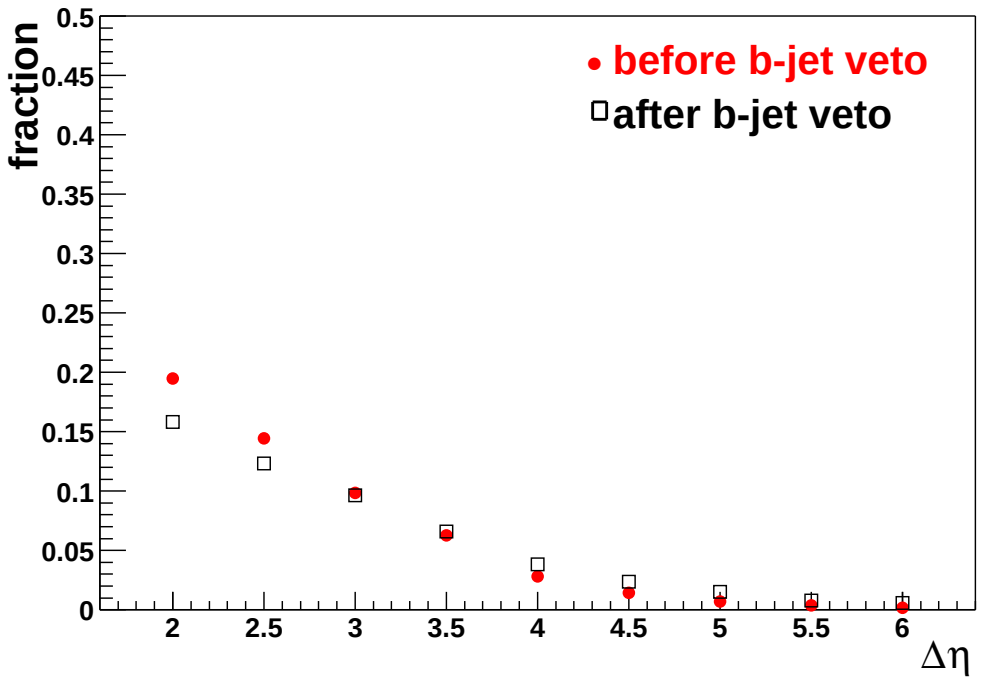

Figure 15: Fraction of events for which both leading and subleading jets are b-jets before and after the application of the central jet veto as a function of $|\Delta\eta|$

The fraction of events for which either the leading or the subleading jet is a b-jet before and after the application of the central jet veto is shown in fig. 16. For $|\Delta\eta| > 3.5$ a $\simeq$ 70% of the events have just one of the 2 leading jets being a b-jet. This fraction is clearly dominated by $t\bar{t}$ + 1jet where the extra jet is hard. The rest of the events were examined and a fraction of 20% were found to have two leading jets that are non-b-jets. These events are dominated by $t\bar{t}$ + 2jets where the two radiated partons are hard. As seen in fig. 16, for $|\Delta\eta| > 3.5$ the $t\bar{t}$ + 2jets contribution is minimum while for larger $|\Delta\eta|$ separation the $t\bar{t}$ + 2jets contribution of the increases. In this respect the choice of $|\Delta\eta| > 3.5$ is optimum since ME calculations are expected to provide a good description of the $t\bar{t}$ + 1jet $P_\perp$ distribution.

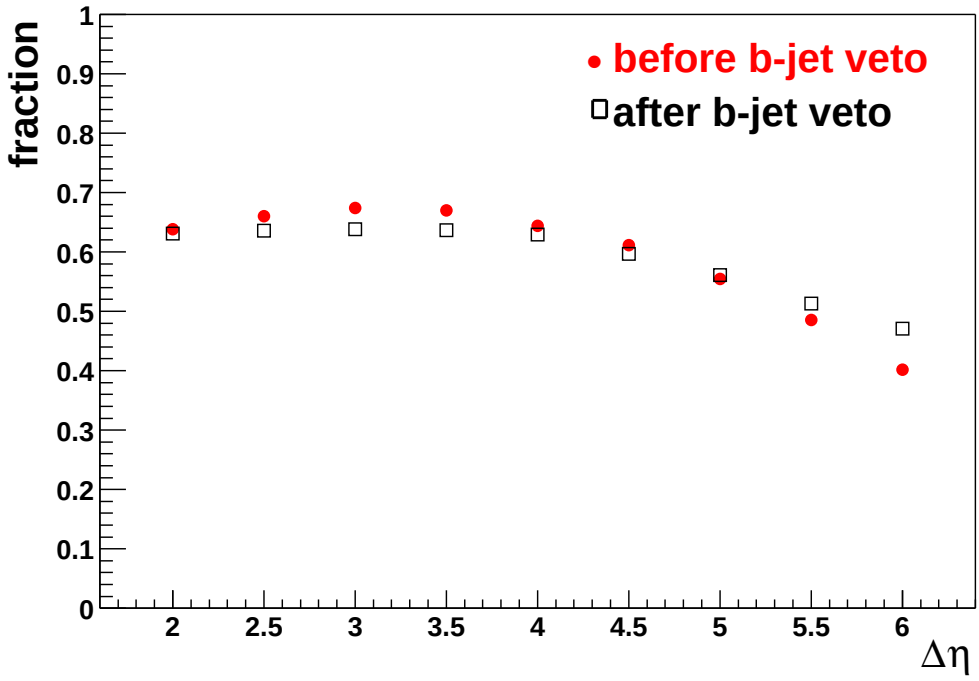

Figure 16: Fraction of events for which either the leading or the subleading jet is a b-jets before and after the application of the central jet veto as a function of $|\Delta\eta|$

The plots presented here show a small dependence of the jet topology on the b-jet veto. Only the third most energetic jet is affected (as expected) but the reduction of the fraction of events for which the third jet is a b-jet is constant as a function of $|\Delta\eta|$. According to these results, it is possible to define a control sample in the early stages of the ATLAS data taking without the central jet veto requirement. One would like to use the part of the phase space which is dominated by $t\bar{t}$ + 1jet and this is clearly the region for which the separation of the tagging jets is $|\Delta\eta| > 3.5$. For a $< 10\%$ systematic error in the normalization of the $t\bar{t}$ + jets background a $\simeq 300 - 500$ pb^{-1} of accumulated luminosity will be needed.

4 Summary

In this note a study of $t\bar{t}$ production at NLO using the MC@NLO Monte-Carlo calculation was presented. A comparison between MC@NLO and standard Monte Carlo programs with LO treatment of the hard process was performed. MC@NLO predicts a dramatic increase of the hard radiation/jets, not associated with the $t\bar{t}$ system, when compared to PYTHIA. MC@NLO was also found to provide a reasonable description of the subleading radiation. As an application, the MC@NLO $t\bar{t}$ production was used to provide a control background sample for the Vector Boson Fusion $H \to WW^* \to ll\nu\nu$ channel. A set of cuts which isolate the part of the $t\bar{t}$ final state which mostly resembles the signature of the signal were found. The background which passes these cuts is dominated by $t\bar{t}$ +1 jet for which ME calculations are expected to provide a good description of the jet $P_\perp$ distribution shape. The sample obtained can be tested against data in the early stages of ATLAS data taking.

References

[1] ATLAS Collaboration, Detector and Physics Performance Technical Design Report, CERN-LHCC/99-14 (1999).

[2] B. Anderson et al., *Phys. Rep.* **97**, 31 (1983);
T. Sjöstrand, *Comp. Phys. Comm.* **82**, 74 (1994);
T. Sjöstrand et al., *Comp. Phys. Comm.* **135**, 238 (2000).

[3] S. Frixione et al., Preprint hep-ph/0305252 (2003);
S. Frixione, B. Webber, Preprint hep-ph/0204244, JHEP 0206:029 (2002).

[4] G. Corcella et al., "HERWIG 6: An event generator for hadron emission reactions with interfering gluons (including supersymmetric processes)", JHEP **0101** (2001) 010;
Preprint hep-ph/00011363 (2000).

[5] F. Maltoni and T. Stelzer, hep-ph/0208156;
T. Stelzer and W.F. Long, *Physics Commun.* **81** 357, (1994);
H. Murayama, I. Watanabe and K. Hagiwara, *KEK-91-11*, (1992).

[6] D. Rainwater and D. Zeppenfeld, *Phys. Rev.* D **60**, 113004 (1999);
N. Kauer et al., *Phys. Lett.* B **503**, 113 (2001).

[7] C. Buttar, K. Jacobs, R. Harper, ATLAS Internal Note, ATL-PHYS-2002-033 (2002);
K. Cranmer, P. McNamara, B. Mellado, W. Quayle, Sau Lan Wu, ATLAS Internal Note, ATL-PHYS-2003-002 (2003);
S. Asai et al., ATLAS Scientific Note, SN-ATLAS-2003-024 (2003).

[8] E. Richter-Was, D. Froidevaux and L. Poggioli, ATLFAST2.0 a Fast Simulation Package for ATLAS, ATLAS Internal Note ATL-PHYS-98-131(1998).

[9] D. Rainwater, PH.D. Thesis Univ. Of Winsconsin 1999.